

Remdesivir induces persistent mitochondrial and structural damage in human induced pluripotent stem cell derived cardiomyocytes

Maxwell Kwok^{1,2}, Carrie Lee^{2,3}, Hung Sing Li^{2,3}, Ruixia Deng^{2,3}, Chantelle Tsoi^{2,3}, Qianqian Ding⁴, Suk Ying Tsang^{4,7}, Kam Tong Leung^{2,8}, Bryan P Yan^{1,9}, Ellen N Poon¹⁻³*

¹Department of Medicine and Therapeutics, ²Hong Kong Hub of Paediatric Excellence (HK HOPE), ³Centre for Cardiovascular Genomics and Medicine, Lui Che Woo Institute of Innovative Medicine, ⁴School of Life Sciences State, ⁵State Key Laboratory of Agrobiotechnology, ⁶Key Laboratory for Regenerative Medicine, Ministry of Education, ⁷Institute for Tissue Engineering and Regenerative Medicine, T, ⁸Department of Paediatrics, ⁹Heart and Vascular Institute, The Chinese University of Hong Kong (CUHK), HKSAR, China

*Correspondence should be addressed to Ellen Ngar-Yun Poon,

E-mail: ellen.poon@cuhk.edu.hk

Tel: (852) 35133164

Add: Laboratory A, 8/F, Tower A, Hong Kong Children's Hospital, 1 Shing Cheong Road, Kowloon Bay, Kowloon, Hong Kong

Short running title: Remdesivir induces persistent cardiotoxicity

Key Words: COVID-19, remdesivir, cardiotoxicity, human pluripotent stem cell derived cardiomyocytes, mitochondria

Original Article, Word Count: 8980

Abstract

Aims: Remdesivir is a prodrug of an adenosine triphosphate analogue and is currently the only drug formally approved for the treatment of hospitalised COVID-19 patients. Nucleoside/nucleotide analogues have been shown to induce mitochondrial damage and cardiotoxicity, and this may be exacerbated by hypoxia, which frequently occurs in severe COVID-19 patients. Although there have been few reports of adverse cardiovascular events associated with remdesivir, clinical data are limited. Here, we investigated whether remdesivir induced cardiotoxicity using an *in vitro* human cardiac model.

Methods and Results: Human induced pluripotent stem cell-derived cardiomyocytes (hiPSC-CMs) were exposed to remdesivir under normoxic and hypoxic conditions to simulate mild and severe COVID-19 respectively. Remdesivir induced mitochondrial fragmentation, reduced redox potential and suppressed mitochondrial respiration at levels below the estimated plasma concentration under both normoxic and hypoxic conditions. Non-mitochondrial damage such as electrophysiological alterations and sarcomere disarray were also observed. Importantly, some of these changes persisted after the cessation of treatment, culminating in increased cell death. Mechanistically, we found that inhibition of DRP1, a regulator of mitochondrial fission, ameliorated the cardiotoxic effects of remdesivir, showing that remdesivir-induced cardiotoxicity was preventable and excessive mitochondrial fission might contribute to this phenotype.

Conclusions: Using an *in vitro* model, we demonstrated that remdesivir can induce cardiotoxicity in hiPSC-CMs at clinically relevant concentrations. These results reveal previously unknown potential side-effects of remdesivir and highlight the importance of further investigations with *in vivo* animal models and active clinical monitoring to prevent lasting cardiac damage to patients.

Translational perspective:

Adult cardiomyocytes have limited ability to regenerate, thus treatment-induced cardiotoxicity can potentially cause irreparable harm. Remdesivir is currently the only FDA approved treatment for COVID-19 but clinical safety data are limited. Using human pluripotent stem cell-derived cardiomyocytes, we revealed that remdesivir induced persistent mitochondrial and structural abnormalities at clinically relevant concentrations. We advise confirmatory experiments in *in vivo* animal models, investigations of cardioprotective strategies, and closer patient monitoring such that treatment-induced cardiotoxicity does not contribute to the long term sequelae of COVID-19 patients.

1 **1. Introduction**

2

3 Coronavirus disease of 2019 (COVID-19), which is caused by severe acute respiratory

4 syndrome coronavirus 2 (SARS-CoV-2), has claimed millions of casualties worldwide. Although

5 COVID-19 primarily affects the respiratory system, cardiac damage is prevalent, occurring in 20-

6 30% of hospitalised patients and contributing to 40% of deaths.¹ The urgency of the COVID-19

7 pandemic has demanded the rapid development of therapeutic strategies. To this end, remdesivir, a

8 compound originally designed for the treatment of Ebola virus disease, has been repurposed for use

9 against COVID-19. Remdesivir has broad spectrum activity against multiple RNA viruses and

10 inhibits SARS-CoV, MERS-CoV, and SARS-CoV-2 *in vitro* and *in vivo*.²⁻⁴ In a double-blind,

11 placebo-controlled multicentre clinical trial, 1062 persons with COVID-19 were randomised to

12 receive a 10-day treatment of remdesivir or placebo.⁵ Patients who received remdesivir experienced

13 a statistically significant decline in the median recovery time to 10 days vs 15 days in the placebo

14 group. Mortality was reduced to 6.7% (remdesivir) vs 11.9% (placebo) by day 15, and 11.4%

15 (remdesivir) vs 15.2% (placebo) by day 29 (hazard ratio, 0.73; 95% CI, 0.52 to 1.03).⁵ These results

16 are consistent with a smaller placebo-controlled trial involving 237 patients which showed a

17 statistically non-significant faster time to clinical improvement in patients who received remdesivir

18 compared to control (21 vs 23 days), particularly in those who received the drug within 10 days of

19 onset of symptoms (16 vs 23 days)⁶. These results are contradictory to the larger open-label WHO

20 Solidarity trial, in which no clinical or survival benefit was observed.⁷ Among patient subgroups,

21 those with moderately severe disease (requiring supplemental oxygen) responded better than those

22 with mild (not requiring oxygen) and severe disease (requiring high flow oxygen or mechanical

23 ventilation).⁵ Serious adverse events were detected at similar rates in the remdesivir treatment vs

24 placebo group.⁵ Remdesivir was first granted emergency use authorisation for the treatment of

25 COVID-19 patients on the May 1, 2020 and was the first and, at the time of writing, the only drug to

26 receive formal approval from the US Food and Drug Administration (FDA) on the Oct 22, 2020 for
27 use in adults and children hospitalised with suspected or laboratory confirmed COVID-19.

28 Remdesivir is a prodrug of an adenosine triphosphate analogue which binds to RNA-
29 dependent RNA polymerase to inhibit viral replication.⁸ Nucleotide/nucleoside analogues are
30 important treatment against RNA viruses but their use have been associated with increased incidences
31 of mitochondrial toxicity, which mainly affects tissues with high energy demand such as the heart.⁹
32 The mitochondria comprise ~30% of the volume of adult cardiomyocytes (CMs), and are critical for
33 cardiac metabolism and apoptosis. Damage to this organelle can therefore severely impair cardiac
34 function. For instance, the clinical development of the nucleotide/nucleoside analogue BMS-986094
35 was terminated due to lethal cardiotoxicity.¹⁰ Toxicity is largely attributed to inhibition of Pol- γ ¹¹ and
36 POLRMT¹², the DNA and RNA polymerases responsible for the synthesis and transcription of
37 mitochondria DNA. Other mechanisms of mitochondrial interference, such as inhibition of and
38 alterations in the expression of mitochondrial genes and proteins¹³, enhanced production of
39 mitochondrial reactive oxygen species¹⁴ have been proposed. Although there have been few reports
40 of adverse cardiac effects related to the use of remdesivir, clinical data are currently limited.

41 Patients with COVID-19 are vulnerable to treatment induced cardiotoxicity due to the high
42 prevalence of cardiovascular damage among these individuals.¹⁵ Many factors may contribute to
43 heart injury including pre-existing cardiovascular co-morbidities^{16, 17}, direct viral infection of CMs¹⁸⁻
44 ²², acute inflammation and myocarditis²³, and hypoxia-induced cardiac damage²⁴. Acute
45 inflammation in the lungs can compromise respiratory function, leading to low oxygen saturation in
46 the blood and hypoxia in the heart. Dyspnea and low oxygen saturation are observed in 50-60% of
47 hospitalised patients with COVID-19, and are associated with greater risk of cardiac damage and poor
48 prognosis.^{25, 26} The heart is metabolically demanding, and is reliant on oxygen to drive oxidative
49 phosphorylation in the mitochondria. Increased cardiometabolic demand associated with systemic
50 infection, coupled with hypoxia caused by acute respiratory illness can disturb the balance between
51 myocardial oxygen demand and supply to result in mitochondrial dysfunction and injury. Remdesivir

52 was initially indicated for use in patients with moderate/severe COVID-19 who requires supplemental
53 oxygen, although this was later broadened to all hospitalised patients. In moderate/severe patients,
54 systemic hypoxemia may damage the heart, and thereby increases susceptibility to the potential
55 adverse effects of remdesivir.

56 Human induced pluripotent stem cells (hiPSCs) can self-renew in culture; their differentiation
57 to the cardiac lineage represents a potentially unlimited source of CMs for disease modelling and
58 cardiotoxicity testing.²⁷⁻²⁹ Human iPSC derived CMs (hiPSC-CMs) spontaneously contract, express
59 genes/proteins associated with cardiac identity and recapitulate key aspects of human cardiac
60 physiology^{27, 30}. Specifically, hiPSC-CMs have been shown to respond to agents which damage the
61 mitochondria and are now an important component of cardiotoxicity testing.^{28, 29, 31} In the context of
62 COVID-19, hiPSC-CMs were recently used to demonstrate direct infection of CMs by SARS-CoV-
63 2.^{18, 19, 22, 32, 33} Sarcomeric disarray, cessation of beating, electrical and contractile disturbances, and
64 apoptosis were observed after infection.^{18, 33} Transcriptional analysis further revealed significant
65 downregulation of genes important for mitochondrial function and oxidative phosphorylation in
66 infected hPSC-CMs.¹⁸ Human iPSC-CMs are therefore a suitable platform for the evaluation of the
67 adverse cardiac effects of COVID-19 treatment.

68 Here, we investigated the cardiotoxic effects of remdesivir by exposing hiPSC-CMs to
69 clinically relevant concentrations of this drug under normoxic and hypoxic conditions to simulate (i)
70 prophylactic use in healthy individuals and treatment for patients with mild COVID-19, and (ii)
71 therapeutic use in patients with severe COVID-19 suffering from pneumonia induced hypoxemia
72 respectively. Remdesivir induced mitochondrial dysfunction in the form of reduced redox potential
73 and respiration, mitochondrial fragmentation, as well as structural abnormalities at concentrations
74 several folds below C_{max} under both normoxic and hypoxic conditions. Importantly, some of these
75 changes persisted after the withdrawal of this drug. Inhibition of mitochondrial fission ameliorated
76 remdesivir induced damage, showing that disturbed mitochondrial dynamics was a mechanistic
77 contributor to the cardiotoxic effects of remdesivir.

78

79 **2. Methods**

80

81 **2.1 Human hPSC culture and cardiac differentiation**

82 We used the hiPSC line AICS-0060-027 (Allen Cell Collection) for our experiments unless otherwise
83 indicated. The cell line is a derivative of the parental line (WTC-11), and contains a mono-allelic
84 mEGFP-tagged MYL2 modification, and was cultured as per instructions from Allen Cell Collection.
85 Cardiac differentiation was performed via the modulation of the WNT signalling pathway.

86

87 **2.2 Evaluation of mitochondrial function**

88 Mitochondrial redox activity was measured using the resazurin-based PrestoBlue assay (Thermo
89 Fisher Scientific, Waltham, MA). Mitochondrial respiration was monitored using a Seahorse
90 extracellular flux analyzer (XFe-96) (Agilent Technologies, CA, USA) using the mito stress assay.
91 For evaluation of mitochondrial and nuclear morphology, cells were incubated with the MitoTracker
92 Deep Red FM dye (Thermo Fisher Scientific) and Hoechst 33342 dye (Thermo Fisher Scientific),
93 and scored. Mitochondrial superoxide (O_2^-) levels were assayed using the MitoSOX™ Red reagent
94 (Thermo Fisher Scientific). Mitochondrial membrane potential ($\Delta\psi_m$) was measured using the
95 tetramethylrhodamine, ethyl ester (TMRE) (Thermo Fisher Scientific).

96

97 **2.3 Action potential measurements**

98 Action potential was measured with ruptured whole-cell patch-clamp.

99

100 Please see supplemental methods for details.

101

102 **3. Results**

103

104 3.1 Remdesivir induced mitochondrial abnormalities in hiPSC-CMs

105 We utilised an hiPSC line (AICS-0060-027) in which the cardiac ventricular marker, MLC2V,
106 is tagged with the eGFP fluorescent reporter. Human iPSC-CMs were generated using an established
107 monolayer differentiation protocol via modulation of the WNT signalling pathway, followed by
108 metabolic selection (Fig. S1A)³⁴. Spontaneous contractions could be observed by days 7-8 of
109 differentiation. Flow cytometry experiments showed that hiPSC cardiac cultures were >95% positive
110 for cardiac Troponin-T, an established marker of CMs, and MLC2V-eGFP⁺ ventricular CMs
111 comprised ~80% of the population at the time of assay (Fig. S1B). CMs were used after day 40 of
112 differentiation, when they assumed an oblong, elongated morphology, with α -actinin and MLC2V-
113 eGFP localised to the Z-disks and A-band respectively (Fig. S1C). Human iPSC-CMs expressed
114 low/high levels of MYH6 and MYH7, commonly associated with structural immaturity/maturity
115 respectively (Fig. S1D).³⁵ These results showed that the hiPSC-CMs had a high degree of structural
116 organisation and were suitable for the modelling of human cardiac dysfunction.

117 Human iPSC-CMs were exposed to remdesivir under normal and hypoxic conditions for three
118 days. Since remdesivir is thought to be most beneficial to patients who receive supplemental oxygen
119 (i.e. mild hypoxia), but not high flow oxygen (severe hypoxia), we chose an oxygen (O₂)
120 concentration of 2.5% to simulate mild hypoxia that did not directly cause cell death but may instead
121 potentiate damage induced by external stimuli. Human iPSC-CMs exposed to 2.5% O₂ were viable,
122 beat and were morphologically indistinguishable from hiPSC-CMs cultured under normoxic (20%
123 O₂) conditions.

124 To determine if remdesivir induced mitochondrial dysfunction, we first compared the redox
125 potential of hiPSC-CMs treated with different doses of this drug under normoxic and hypoxic
126 conditions. The 50% effective concentration (EC₅₀) of remdesivir *in vitro* is in the (sub)micromolar
127 range while the C_{max} of remdesivir in healthy volunteers is 9.0 and 4.3 μ M on day 1 and 5 of
128 treatment respectively.³⁶ A dose range of 0.1-12.5 μ M was chosen to represent clinically relevant
129 concentrations of remdesivir for cardiotoxicity evaluations. Redox potential is mostly driven by the

130 proton gradient in the mitochondria and is often used as an indicator of metabolic activity in this
131 organelle. Remdesivir dose-dependently reduced redox potential under normoxic and hypoxic
132 conditions (Fig. 1A). While remdesivir had negligible effects at low doses (0.1 μ M and 0.5 μ M), it
133 significantly decreased redox activity at 2.5 μ M and 12.5 μ M by $21.0\pm 3.9\%$ and $35.9\pm 4.0\%$ under
134 normoxic, and by $22.5\pm 5.4\%$ and $28.7\pm 6.9\%$ under hypoxic conditions respectively.

135 Next, we tested the effect of remdesivir on mitochondrial respiration, which is critical for
136 cardiac metabolism. Seahorse metabolic flux assay showed that remdesivir repressed respiration in a
137 dose-dependent manner (Fig. 1B). Under normoxic conditions, remdesivir significantly reduced basal
138 respiration and ATP production by $59.8\pm 5.7\%$ and $68.3\pm 8.3\%$ respectively when applied at 2.5 μ M.
139 Under hypoxic conditions, remdesivir significantly reduced basal respiration by $33.3\pm 6.1\%$ and
140 $36.3\pm 8.7\%$ at 0.5 μ M and 2.5 μ M; maximal respiration at $37.7\pm 8.0\%$ at 2.5 μ M; and ATP production
141 at $24.9\pm 5.9\%$ and $37.5\pm 8.4\%$ at 0.1 μ M and 0.5 μ M. Remdesivir at 12.5 μ M produced highly variable
142 effects of oxygen consumption.

143 Mitochondrial dynamics constitutes part of the quality control process of this organelle and is
144 maintained by a balance between fusion and fission, which promote the elongation and fragmentation
145 of mitochondria, respectively.^{37, 38} Since mitochondrial dynamics is frequently disturbed by
146 cardiotoxins, we investigated whether remdesivir altered mitochondrial morphology. Fluorescence
147 imaging of mitochondrial dye revealed three patterns of mitochondrial morphologies among hiPSC-
148 CMs (Fig. 1C and S2A). The first consisted of densely organised, elongated mitochondrial networks
149 spread throughout the cytoplasm and this is considered to represent a healthy balance of fission and
150 fusion. The second had punctate, fragmented mitochondria consistent with increased fission. The last
151 had mitochondria located around the nucleus, also suggestive of an imbalance towards increased
152 fission. All hiPSC-CM samples exhibited a mixture of the three phenotypes, but in different
153 proportions. Control, normoxic hiPSC-CMs primarily had an elongated mitochondrial network while
154 remdesivir induced mitochondrial fragmentation in a dose-dependent manner (Fig 1C). Under
155 normoxic conditions, the proportion of cells with elongated mitochondria significantly decreased

156 from $65.1\pm 6.8\%$ in control hiPSC-CMs to $43.9\pm 7.5\%$, $27.3\pm 6.0\%$, and $13.4\pm 5.0\%$ upon treatment
157 with increasing doses of remdesivir at 0.5, 2.5 μM and 12.5 μM respectively, and this was
158 accompanied by a corresponding increase in the proportion of cells with punctate, fragmented
159 mitochondria from $21.0\pm 5.9\%$ to $44.4\pm 7.1\%$, $57.3\pm 7.2\%$ and $64.4\pm 9.5\%$. Similarly, hypoxia decreased
160 the prevalence of elongated mitochondria in favour of punctate mitochondria and this worsened with
161 increasing doses of remdesivir. The proportion of elongated mitochondria significantly decreased
162 from $45.1\pm 7.8\%$ in control hPSC-CMs to $18.7\pm 3.0\%$ and $17.8\pm 4.2\%$ upon treatment with 2.5 μM and
163 12.5 μM of remdesivir, while the proportion of punctate mitochondria rose from $37.3\pm 6.1\%$ in
164 control, to $64.4\pm 4.1\%$ and $58.9\pm 8\%$ at the same doses. The proportion of cells with perinuclear
165 mitochondria was similar in all samples. Consistent with these results, immunostaining for TOM20,
166 a protein present in the outer mitochondrial membrane that is commonly used as a marker of
167 mitochondria, also revealed mitochondrial fragmentation in hiPSC-CMs treated with remdesivir (Fig.
168 S3A). The mitochondrial mass of hiPSC-CMs, as measured by the intensity of mitochondrial dye
169 staining, was not statistically different among different groups (Fig. S4A), showing that remdesivir
170 promoted mitochondrial fragmentation but did not alter mitochondrial mass in hiPSC-CMs.

171 To determine if increased oxidative stress contributed to the toxic effects of remdesivir, the
172 level of reactive oxygen species (ROS) in the form of mitochondrial superoxide was measured using
173 the MitoSox red dye and was found to be similar in control and treated hiPSC-CMs (Fig. S4B). These
174 results were further confirmed using the CellRox dye, an indicator of ROS in the cytoplasm as well
175 as the mitochondria (data not shown).

176 We next tested whether remdesivir induced the depolarisation of the mitochondrial membrane
177 potential ($\Delta\psi\text{m}$), which is commonly considered to be a prelude to irreversible apoptosis and cell
178 death. No statistically significant decrease in $\Delta\psi\text{m}$ was detected (Fig. S4C).

179 To investigate if remdesivir disturbed the expression of genes important for mitochondrial
180 function, we measured the mRNA levels of genes encoding components of electron transport chain
181 (ETC) encompassing the mitochondrial complex I (MT-ND1 and MT-ND5), II (SDHA), IV

182 (COX6A2) and V (ATP6), as well as a non-ETC gene encoding a mediator of fatty acid β -oxidation
183 in the mitochondria (ACADVL) (Fig. 2). With the exception of SDHA, remdesivir dose-dependently
184 and significantly reduced the expression of ETC genes including ND1, ND5, COX6A2 and ATP6,
185 while ACADVL mRNA levels were similar among all samples. Of the ETC genes, MT-ND1, MT-
186 ND5 and ATP6 are encoded by the mitochondrial genome, while COX6A2 and SDHA are encoded
187 by the nuclear genome. Thus, the effect of remdesivir was not limited to mitochondrial- or nuclear-
188 encoded genes. Overall, the general repression of ETC gene transcripts was consistent with and might
189 contribute to the reduced redox potential and mitochondrial respiration detected (Fig 1A and B).

190

191 **3.2 Remdesivir induced structural abnormalities but not cell death**

192 In addition to mitochondrial dysfunction, non-mitochondrial damage was observed in
193 remdesivir-treated cells and manifested as perturbations in sarcomeric arrangement. In control hiPSC-
194 CMs, eGFP-tagged MLC2V assumed a densely-packed striated appearance along myofilaments
195 which spanned the entire cell, reflecting its localisation to the thick filaments of sarcomeres (Fig S1C
196 and 3A). Low doses of remdesivir (0.1 and 0.5 μ M) did not have any noticeable effect under normoxic
197 conditions, but 0.5 μ M of remdesivir under hypoxia induced the thinning and truncation of myofibrils.
198 Human iPSC-CMs treated with 2.5 and 12.5 μ M of remdesivir had greatly disorganised myofibrils
199 under both normoxic and hypoxic conditions. While cells with striated structures could still be found,
200 sparse and truncated myofibrils, and patchy MLC2V-eGFP signal with no or poorly discernible
201 organisation were common. Similarly, immunostaining against α -actinin, a protein located at the Z-
202 lines of CMs, also revealed severe disorganisation and areas of barely detectable signal in hiPSC-
203 CMs treated with 2.5 and 12.5 μ M of remdesivir (Fig. S3B).

204 We next tested if remdesivir induced apoptosis or cell death in hiPSC-CM cultures. Nuclear
205 condensation is a sign of apoptosis and manifest as brightly-stained, small and 'condensed' nuclei
206 (Fig. S2B). Staining with the Hoescht nuclear dye did not reveal any significant increase in the
207 number of condensed nuclei following remdesivir treatment (Fig 3B). Consistently, nuclear area and

208 staining intensity were similar in control and remdesivir treatment groups irrespective of dose and
209 normoxia/hypoxia (Fig. S5). No significant difference in cell number was observed among all
210 samples, demonstrating the absence of significant cell detachment (Fig. S5). We thus concluded that
211 remdesivir did not significantly induce cell death in hiPSC-CM cultures.

212

213 **3.3 Remdesivir altered the electrophysiological properties of hiPSC-CMs**

214 In addition to mitochondrial toxicity, we also tested if remdesivir disturbed the
215 electrophysiological properties of hiPSC-CMs. Single cell patch clamp analysis showed that
216 remdesivir (2.5 μM) significantly reduced spontaneous firing frequency (Control 0.89 ± 0.14 vs
217 remdesivir 0.36 ± 0.07 Hz) and the diastolic depolarisation rate (Control 20.32 ± 3.77 vs remdesivir
218 7.74 ± 1.19 mV/s), and tended to decrease the maximum depolarisation rate (Control 40.94 ± 7.42 vs
219 remdesivir 21.7 ± 6.38 mV/s) (Fig. 4). The action potential amplitude, and maximal diastolic potential
220 were similar in control and hiPSC-CMs treated with remdesivir.

221

222 **3.4 Remdesivir induced persistent cardiac damage**

223 Our results so far demonstrated that remdesivir caused mitochondrial, structural and
224 electrophysiological abnormalities, but significant changes associated with irreversible damage such
225 as $\Delta\psi\text{m}$ depolarisation and nuclear condensation were not observed. We therefore asked if damage
226 induced by remdesivir was transient and reversible. To address this, hiPSC-CMs were exposed to
227 remdesivir as described previously, followed by ‘recovery’ for 3 days in media devoid of this drug
228 under normoxic conditions to simulate patient recovery after the cessation of remdesivir treatment
229 (Fig. 5A). Remdesivir dose-dependently altered redox potential under normoxic and hypoxic
230 conditions. It significantly decreased redox potential by $31.1\pm 5.3\%$ and $44.1\pm 8.1\%$ at 2.5 μM and
231 12.5 μM under normoxic condition, and by $41.0\pm 8.7\%$ and $54.6\pm 8.5\%$ under hypoxic conditions (Fig.
232 5B).

233 We also evaluated whether remdesivir-induced mitochondrial fragmentation was reversed
234 upon recovery. While low dose of remdesivir (0.5 μM) altered mitochondrial morphology
235 immediately after treatment (Fig. 1C), no significant difference was detected between control and
236 treated cells upon recovery (Fig. 5C). By contrast, the mitochondria of hiPSC-CMs treated with
237 higher doses of this drug (2.5 μM and 12.5 μM) remained more fragmented than control. The
238 proportion of cells with elongated mitochondria decreased from $40.1\pm 4.5\%$ in control CMs to
239 $17.2\pm 6.6\%$ and $7.3\pm 3.8\%$ in hiPSC-CMs treated with 2.5 μM and 12.5 μM of remdesivir respectively.
240 Similar trends were observed under hypoxic conditions: showing a decrease in elongated
241 mitochondria from $47.4\pm 4.9\%$ in control to $19.7\pm 2.5\%$ and $4.6\pm 2.1\%$ with 2.5 μM and 12.5 μM
242 remdesivir, and this was accompanied by a corresponding increase in the proportion of cells with
243 punctate mitochondria from $46.1\pm 3.8\%$ to $66.1\pm 1.1\%$ and $65.5\pm 6.6\%$. The proportion of cells with
244 perinuclear mitochondria increased from $6.5\pm 1.5\%$ in control to $29.9\pm 5.7\%$ with 12.5 μM remdesivir,
245 demonstrating persistent mitochondrial damage (Fig. 5C). Apart from mitochondrial changes,
246 structural alterations also persisted beyond the three-day treatment period. Cells treated with 2.5 μM
247 and 12.5 μM of remdesivir showed disorganised sarcomeric arrangement analogous to the patterns
248 seen immediately after treatment (Fig. 3A and 5D).

249 We evaluated the prevalence of nuclear condensation as a surrogate for apoptosis and cell
250 death. Although no significant increase in nuclear condensation was seen immediately after three
251 days of treatment (Fig. 3B), a dose dependent increase in the proportion of condensed nuclei was
252 observed in hiPSC-CMs three days after they were treated with 2.5 μM and 12.5 μM of remdesivir
253 (Fig. 5E). The same trend was also observed with the TUNEL assay, which detects DNA breaks,
254 further confirming that remdesivir-induced cardiotoxicity can ultimately lead to increased apoptosis
255 (Fig. S6).

256 Lastly, we extended our 'recovery' period to 14 days and asked if mitochondrial and structural
257 abnormalities could still be observed. Human iPSC-CMs treated with remdesivir exhibited
258 significantly reduced redox potential of $35.4\pm 6.4\%$ and $43.0\pm 5.6\%$ at 2.5 μM and 12.5 μM under

259 normoxic and $22.7\pm 3.8\%$ at $2.5\ \mu\text{M}$ under hypoxic conditions, compared to control (Fig. S7A).
260 Mitochondrial fragmentation and sarcomeric disarray were also apparent, showing that remdesivir
261 treatment had a long term detrimental impact on hiPSC-CMs (Fig. S7B and C).

262 In summary, remdesivir induced mitochondrial and structural damage which persisted beyond
263 the treatment period, culminating in increased cell death.

264

265 **3.5 Remdesivir-induced cardiotoxicity could be ameliorated by an inhibitor of** 266 **mitochondrial fission**

267 Given the extensive mitochondrial fragmentation observed in remdesivir treated hiPSC-CMs,
268 we proposed that excessive mitochondrial fission might underlie the cardiotoxic effects induced by
269 this drug, and that the inhibition of DRP1^{38, 39}, a master regulator of mitochondrial fission, could
270 protect against remdesivir. We tested this by applying mdivi-1, which is a well-established inhibitor
271 of DRP1⁴⁰, to hiPSC-CMs. Human iPSC-CMs treated with mdivi-1 alone had similar redox potential,
272 exhibited elongated mitochondria and organised sarcomeres comparable to control cells (Fig. 6A and
273 S8A). Mdivi-1 has been shown to have an IC₅₀ of $10\ \mu\text{M}$ for mitochondrial fragmentation in human
274 cells⁴¹. We therefore tested the ability of $5\ \mu\text{M}$, $15\ \mu\text{M}$, $50\ \mu\text{M}$ of mdivi-1 to repress remdesivir
275 induced mitochondrial fragmentation. $15\ \mu\text{M}$ of remdesivir was found to be most consistently
276 protective and was used for subsequent experiments (Fig. S8B). Co-treatment of mdivi-1 with 2.5
277 μM remdesivir significantly promoted the formation of elongated mitochondria under normoxic
278 conditions compared to cells treated with remdesivir alone (Fig. 6B). Mdivi-1 treatment also produced
279 a corresponding decrease in the proportion of cells with punctate mitochondria under hypoxia. Similar
280 observations were made using immunostaining with anti-TOM20 antibody (Fig. S3A), further
281 confirming the protective effects of mdivi-1. However, at $12.5\ \mu\text{M}$ remdesivir, mdivi-1 could only
282 significantly protect hiPSC-CMs under hypoxic but not normoxic conditions.

283 We next tested if preventing mitochondrial fragmentation with mdivi-1 could normalise redox
284 potential in hiPSC-CMs. Under both normoxic and hypoxic conditions, mdivi-1 restored redox

285 potential in hiPSC-CMs treated with 2.5 μM of remdesivir to near control levels (Fig. 6A). However,
286 the same trend was not observed at 12.5 μM of remdesivir, at which mdivi-1 did not have noticeable
287 effect.

288 The structural abnormalities induced by remdesivir could also be ameliorated by mdivi-1.
289 Mdivi-1 improved the sarcomere arrangement of CMs treated with 2.5 μM , and 12.5 μM of
290 remdesivir (Fig. 6C). Myofibrils were more densely packed, and MLC2V-eGFP signal was more
291 striated with mdivi-1 co-treatment than remdesivir alone.

292 Lastly, we measured the level of DRP1 mRNA and protein in control and remdesivir-treated
293 cells to test if remdesivir directly altered DRP1 expression. Although DRP1 mRNA showed a dose-
294 dependent and significant increase in cells treated with remdesivir (Fig. S8C), there was no noticeable
295 change in protein expression (Fig. S8D). These results showed that while DRP1 participated in the
296 pathogenesis of remdesivir induced cardiotoxicity, remdesivir did not promote mitochondrial fission
297 via upregulation of this protein.

298 In summary, our results showed that remdesivir induced cardiotoxicity was preventable and
299 could be ameliorated by mdivi-1 *in vitro*, and identified excessive mitochondrial fission to be a
300 mechanistic contributor to this phenotype.

301

302 **3.6 The cardiotoxic effect of remdesivir is not cell-line specific**

303 Key findings were validated in a second hiPSC line, MDI-C16, showing that our results are
304 not cell line dependent. These experiments confirmed reduced redox potential (Fig. S9A) and
305 mitochondrial fragmentation (Fig. S9B) upon remdesivir treatment. These changes persisted for at
306 least three days after remdesivir treatment (Fig. S10) and mdivi-1 ameliorated the toxicity induced
307 by remdesivir (Fig. S9C).

308

309 **4. Discussion**

310 Remdesivir is a nucleotide analogue effective against COVID-19, but its potential to cause
311 cardiotoxicity is unclear. Using an *in vitro* hiPSC-CM model, we showed that remdesivir induced
312 cardiotoxicity at clinically relevant concentrations under normoxic and hypoxic conditions.
313 Mitochondrial dysfunctions and sarcomere disarray were detected, and they persisted after cessation
314 of treatment. Consistent with recent clinical reports of serious bradycardia, remdesivir also perturbed
315 electrophysiological properties of hiPSC-CMs. This is the first report of adverse and persistent
316 cardiac effects associated with remdesivir at clinically relevant concentrations and highlights the
317 importance of cardiac monitoring in patients treated with this drug. Importantly, inhibition of
318 mitochondrial fission protected against mitochondrial fragmentation, normalised redox potential and
319 prevented sarcomere disarray, showing that remdesivir induced cardiotoxicity can be ameliorated.

320 The efficacy of remdesivir against COVID-19 has been demonstrated in many *in vitro* and *in*
321 *vivo* studies.^{2,3} Remdesivir is effective *in vitro* in the sub-micromolar range: it blocked SARS-CoV-
322 2 infection in African green monkey kidney Vero E6 cells with an EC50 and EC90 of 0.77 μM and
323 1.76 μM respectively,³ and in human airway epithelial cells, at an IC50 of 0.069 μM .⁴² Remdesivir
324 is also efficacious in randomised clinical trials and shortened time to recovery.⁵ In light of these
325 findings, remdesivir received authorisation from the US FDA for use in hospitalised patients with
326 COVID-19 with a standard dose of 200 mg, followed by daily doses of 100 mg for 4 or 9 days. In
327 healthy adult volunteers receiving a similar dose regimen, and the peak plasma concentrations were
328 5.4 $\mu\text{g/mL}$ (9.0 μM) on day 1 and 2.6 $\mu\text{g/mL}$ (4.3 μM) on day 5.³⁶ Thus both the EC50 and the Cmax
329 of remdesivir are within the dosage range tested in this study (0.1-12.5 μM). We first detected
330 increased mitochondrial fragmentation at 0.5 μM but these perturbations did not persist. On the other
331 hand, multiple features of mitochondrial and sarcomeric abnormalities were observed at ≥ 2.5 μM
332 under normoxic and hypoxic conditions, which is 3.6 and 1.7 fold below Cmax in patients on day 1
333 and 5 of treatment. Importantly, these abnormalities persisted after cessation of treatment,
334 culminating in increased cell death.

335 Mitochondrial toxicity of remdesivir has been demonstrated in two human intestinal (HT29
336 and HCT116) and two human liver cell lines (HepG2 and PLC/PRF/5) at high doses of 10 or 20 μM .⁴³
337 Conversely, a recent report evaluated the effect of remdesivir using a panel of cell lines and primary
338 cells, and concluded that remdesivir had a low potential to elicit off-target toxicity, although
339 significant cell line specific differences were noted.⁴⁴ Neither of the two reports included CMs. Ours
340 is the first report of persistent mitochondrial toxicity in CMs at clinically relevant concentrations. By
341 systematically evaluating the mitochondrial phenotype of remdesivir treated cells, we showed that
342 remdesivir primarily induced mitochondrial fragmentation, suppressed mitochondrial respiration and
343 reduced redox potential. Mitochondrial damage may occur via various mechanisms. The toxicity of
344 ribonucleoside/nucleotide analogues has largely been attributed to inhibition of POLRMT¹¹, the RNA
345 polymerase responsible for the transcription of mitochondria DNA. However, purified human
346 mitochondrial RNA polymerase has been shown to effectively discriminate against remdesivir-
347 triphosphate with a selectivity value of ~ 500 -fold,⁴⁵ and remdesivir triphosphate was found to have
348 negligible effect on key human DNA and RNA polymerases⁴⁴, suggesting that inhibition of the latter
349 is unlikely to be a major contributor of the cardiotoxic effects of remdesivir. Instead, we identified
350 excessive mitochondrial fission to be a critical driver of the remdesivir induced abnormalities, since
351 the inhibition of the former with a small molecule inhibitor, mdivi-1, reduced mitochondrial
352 fragmentation, normalised redox potential and improved sarcomeric arrangement in cells treated with
353 2.5 μM of remdesivir. Excessive mitochondrial fragmentation has previously been shown to
354 contribute to a range of cardiac disorders and mdivi-1 is cardioprotective in the settings of
355 doxorubicin induced cardiotoxicity,⁴⁶ ischemia-reperfusion injury,^{47, 48} and pressure overload induced
356 heart failure.⁴⁹ Here we provide important proof-of-principle that cardioprotective strategies (such as
357 mdivi-1) can be employed to at least partially protect CMs against the cardiotoxic effects of
358 remdesivir. It is possible that additional factors contribute to the cardiotoxicity of remdesivir at
359 extremely high doses and this may explain the lesser ability of mdivi-1 to protect against remdesivir
360 at 12.5 μM .

361 We initially reasoned that hypoxia might potentiate the mitochondrial toxicity induced by
362 remdesivir; instead remdesivir induced similar level of toxicity under normoxic and hypoxic
363 conditions. These unexpected findings may relate to the severity of hypoxia used in the study. There
364 is a paucity of data that directly correlates oxygen saturation *in vivo* with oxygen concentration *in*
365 *vitro*. Furthermore, COVID-19 patients exhibit highly diverse oxygen saturation ranging from normal
366 (>95%), to very low (<70%).⁵⁰ It is therefore difficult to choose an O₂ concentration *in vitro* to
367 represent all patients. Since remdesivir was found to be most effective in patients with mild hypoxia
368 (i.e. requiring oxygen supplementation but not mechanical ventilation)⁵, we chose an oxygen (O₂)
369 concentration of 2.5% to simulate mild hypoxia that did not directly cause cell death. It is possible
370 that the relatively mild conditions used was not enough to exacerbate the effects of remdesivir.

371 In addition to mitochondrial damage, single cell patch clamp analysis revealed
372 electrophysiological alterations in hiPSC-CMs treated with 2.5 μM of remdesivir. Specifically,
373 remdesivir decreased firing frequency and this is consistent with a previous examination of remdesivir
374 using multi-electrode array analysis, which showed prolonged field potential duration and reduced
375 beating rates.³² Both our observations are in line with recent reports of bradycardia observed in
376 patients.^{51, 52}

377 Remdesivir was previously considered to be safe in animal studies and in clinical trials.
378 Remdesivir has been associated with a slight increase in the risk of cardiac arrest (1.9% vs 1.4%) and
379 serious atrial fibrillation (0.9% vs 0.2%) compared to placebo in one clinical study⁵, but the Solidarity
380 trial by the WHO showed similar rates of cardiac death (0.3% vs 0.4%).⁷ Adverse cardiovascular
381 events and evaluations of cardiac stress markers were not reported in two other clinical studies.^{53, 54}
382 Due to the low numbers of cardiovascular incidences reported, it is unclear whether the difference in
383 cardiac outcome observed between remdesivir and placebo groups are significant, but immediate,
384 overt cardiotoxicity was not apparent. There are potentially multiple reasons for the dichotomy
385 between our study and currently available clinical data. Firstly, we utilised *in vitro* derived hiPSC-
386 CMs, which may be immature and may not respond in the same manner as human adult CMs.⁵⁵⁻⁵⁸

387 Secondly, the cardiotoxicity of remdesivir initially manifests as mitochondrial and structural
388 abnormalities without overt cell death during the treatment period, and may not be immediately
389 apparent in clinical trials, which primarily report acute clinical adverse events. Thirdly and
390 importantly, pre-existing cardiac co-morbidities, and direct cardiac damage caused by COVID-19
391 may mask any adverse effects of remdesivir. Further investigations in animal models or in patients
392 would be critical to confirm cardiotoxicity *in vivo*. For clinical monitoring, high sensitivity troponin
393 measurements, which can detect the death of CMs, may be informative during and after treatment.
394 Cardiovascular magnetic resonance have already been used to reveal lower left ventricular ejection
395 fraction, higher left ventricle volumes, and raised native T1 and T2 in patients recovered from
396 COVID-19⁵⁹ and may aid in the detection of subtle changes in cardiac function induced by
397 remdesivir.

398 Remdesivir is currently used clinically at a concentration that far exceeds its effective
399 concentration *in vitro*. Remdesivir can inhibit SARS-CoV-2 in African green monkey kidney Vero
400 E6 and human airway epithelial cells with an EC/IC50 of 0.77 μM and 0.069 μM . respectively^{3, 42}.
401 Similarly, recent studies in hPSC-CMs also demonstrated efficacy of remdesivir at 0.2-0.6 μM .^{22, 32}
402 While remdesivir induced cardiotoxicity $\geq 2.5 \mu\text{M}$, we did not observe persistent functional alterations
403 at low concentration of this drug closer to its *in vitro* effective dose (0.1 μM and 0.5 μM). It may be
404 beneficial to assess the *in vivo* efficacy of this drug at lower doses to minimise adverse effects.
405 Consistent with this, clinical trials comparing 5 or 10 days of remdesivir treatment either showed that
406 there was no statistically significant difference in clinical outcome, or that the 5-day regimen was
407 slightly superior.^{53, 54} A careful titration of dose and duration, and alternate formulations of
408 remdesivir⁶⁰ may help to balance antiviral efficacy with cardiotoxic risks.

409 Despite the limitations of our model, the demonstration of persistent cardiotoxicity at
410 clinically relevant concentrations highlight the need for further investigations of cardiotoxicity in *in*
411 *vivo* animal models, and clinical studies. Adult CMs have limited ability to regenerate, thus treatment-
412 induced cardiotoxicity can potentially cause irreparable harm to patients already made vulnerable by

413 cardiovascular co-morbidities and cardiac damage caused by viral infection. Functional cardiac
414 monitoring in the clinic are warranted such that cardiotoxicity does not contribute to the long term
415 sequelae of COVID-19 patients.

416

417 **Funding**

418 This work was supported by funding from the Improvement on competitiveness in hiring new
419 faculties funding scheme [4930915] and the Direct grant [4054538] from the Chinese University of
420 Hong Kong to E.N.P.

421

422 **Data availability**

423 The data underlying this article are available in the article and in its online supplementary material.

424

425 **Author Contribution Statement**

426 E.N.P conceived the study. M.K. maintained and differentiated hiPSCs, and performed most of the
427 cell biology experiments. C.L performed immunostaining, microscopy and analysis. C.T and R.D.
428 performed image analysis. H.S.L. and K.T.L. performed qPCR and Western blotting experiments.
429 Q.D and S.Y.T performed electrophysiological experiments. All members including M.K., C.L.,
430 H.S.L., C.T., R.D., Q.D, S.Y.T, K.T.L, B.P.Y and E.N.P prepared and wrote the manuscript.

431

432 **Conflict of Interest**

433 None declared.

434

435 **References**

- 436 1. Madjid M, Safavi-Naeini P, Solomon SD, Vardeny O. Potential Effects of Coronaviruses on
437 the Cardiovascular System: A Review. *JAMA Cardiol* 2020.
- 438 2. Williamson BN, Feldmann F, Schwarz B, Meade-White K, Porter DP, Schulz J, van
439 Doremalen N, Leighton I, Yinda CK, Perez-Perez L, Okumura A, Lovaglio J, Hanley PW,
440 Saturday G, Bosio CM, Anzick S, Barbican K, Cihlar T, Martens C, Scott DP, Munster VJ,
441 de Wit E. Clinical benefit of remdesivir in rhesus macaques infected with SARS-CoV-2.
442 *Nature* 2020.
- 443 3. Wang M, Cao R, Zhang L, Yang X, Liu J, Xu M, Shi Z, Hu Z, Zhong W, Xiao G.
444 Remdesivir and chloroquine effectively inhibit the recently emerged novel coronavirus
445 (2019-nCoV) in vitro. *Cell Res* 2020;**30**:269-271.
- 446 4. Pruijssers AJ, George AS, Schafer A, Leist SR, Gralinski LE, Dinnon KH, 3rd, Yount BL,
447 Agostini ML, Stevens LJ, Chappell JD, Lu X, Hughes TM, Gully K, Martinez DR, Brown
448 AJ, Graham RL, Perry JK, Du Pont V, Pitts J, Ma B, Babusis D, Murakami E, Feng JY,
449 Bilello JP, Porter DP, Cihlar T, Baric RS, Denison MR, Sheahan TP. Remdesivir Inhibits
450 SARS-CoV-2 in Human Lung Cells and Chimeric SARS-CoV Expressing the SARS-CoV-2
451 RNA Polymerase in Mice. *Cell reports* 2020;**32**:107940.
- 452 5. Beigel JH, Tomashek KM, Dodd LE, Mehta AK, Zingman BS, Kalil AC, Hohmann E, Chu
453 HY, Luetkemeyer A, Kline S, Lopez de Castilla D, Finberg RW, Dierberg K, Tapson V,
454 Hsieh L, Patterson TF, Paredes R, Sweeney DA, Short WR, Touloumi G, Lye DC,
455 Ohmagari N, Oh MD, Ruiz-Palacios GM, Benfield T, Fatkenheuer G, Kortepeter MG,
456 Atmar RL, Creech CB, Lundgren J, Babiker AG, Pett S, Neaton JD, Burgess TH, Bonnett T,
457 Green M, Makowski M, Osinusi A, Nayak S, Lane HC, Members A-SG. Remdesivir for the
458 Treatment of Covid-19 - Final Report. *N Engl J Med* 2020.
- 459 6. Wang Y, Zhang D, Du G, Du R, Zhao J, Jin Y, Fu S, Gao L, Cheng Z, Lu Q, Hu Y, Luo G,
460 Wang K, Lu Y, Li H, Wang S, Ruan S, Yang C, Mei C, Wang Y, Ding D, Wu F, Tang X,

- 461 Ye X, Ye Y, Liu B, Yang J, Yin W, Wang A, Fan G, Zhou F, Liu Z, Gu X, Xu J, Shang L,
462 Zhang Y, Cao L, Guo T, Wan Y, Qin H, Jiang Y, Jaki T, Hayden FG, Horby PW, Cao B,
463 Wang C. Remdesivir in adults with severe COVID-19: a randomised, double-blind, placebo-
464 controlled, multicentre trial. *Lancet* 2020;**395**:1569-1578.
- 465 7. Consortium WHOIST, Pan H, Peto R, Henao-Restrepo AM, Preziosi MP, Sathiyamoorthy V,
466 Abdool Karim Q, Alejandria MM, Hernandez Garcia C, Kieny MP, Malekzadeh R, Murthy
467 S, Reddy KS, Roses Periago M, Abi Hanna P, Ader F, Al-Bader AM, Alhasawi A, Allum E,
468 Alotaibi A, Alvarez-Moreno CA, Appadoo S, Asiri A, Aukrust P, Barratt-Due A, Bellani S,
469 Branca M, Cappel-Porter HBC, Cerrato N, Chow TS, Como N, Eustace J, Garcia PJ,
470 Godbole S, Gotuzzo E, Griskevicius L, Hamra R, Hassan M, Hassany M, Hutton D,
471 Irmansyah I, Jancoriene L, Kirwan J, Kumar S, Lennon P, Lopardo G, Lydon P, Magrini N,
472 Maguire T, Manevska S, Manuel O, McGinty S, Medina MT, Mesa Rubio ML, Miranda-
473 Montoya MC, Nel J, Nunes EP, Perola M, Portoles A, Rasmin MR, Raza A, Rees H, Reges
474 PPS, Rogers CA, Salami K, Salvadori MI, Sinani N, Sterne JAC, Stevanovikj M, Tacconelli
475 E, Tikkinen KAO, Trelle S, Zaid H, Rottingen JA, Swaminathan S. Repurposed Antiviral
476 Drugs for Covid-19 - Interim WHO Solidarity Trial Results. *N Engl J Med* 2021;**384**:497-
477 511.
- 478 8. Yin W, Mao C, Luan X, Shen DD, Shen Q, Su H, Wang X, Zhou F, Zhao W, Gao M, Chang
479 S, Xie YC, Tian G, Jiang HW, Tao SC, Shen J, Jiang Y, Jiang H, Xu Y, Zhang S, Zhang Y,
480 Xu HE. Structural basis for inhibition of the RNA-dependent RNA polymerase from SARS-
481 CoV-2 by remdesivir. *Science* 2020;**368**:1499-1504.
- 482 9. Apostolova N, Blas-Garcia A, Esplugues JV. Mitochondrial interference by anti-HIV drugs:
483 mechanisms beyond Pol-gamma inhibition. *Trends in pharmacological sciences*
484 2011;**32**:715-725.
- 485 10. Ahmad T, Yin P, Saffitz J, Pockros PJ, Lalezari J, Shiffman M, Freilich B, Zamparo J,
486 Brown K, Dimitrova D, Kumar M, Manion D, Heath-Chiozzi M, Wolf R, Hughes E, Muir

- 487 AJ, Hernandez AF. Cardiac dysfunction associated with a nucleotide polymerase inhibitor
488 for treatment of hepatitis C. *Hepatology* 2015;**62**:409-416.
- 489 11. Lewis W, Simpson JF, Meyer RR. Cardiac mitochondrial DNA polymerase-gamma is
490 inhibited competitively and noncompetitively by phosphorylated zidovudine. *Circ Res*
491 1994;**74**:344-348.
- 492 12. Feng JY, Xu Y, Barauskas O, Perry JK, Ahmadyar S, Stepan G, Yu H, Babusis D, Park Y,
493 McCutcheon K, Perron M, Schultz BE, Sakowicz R, Ray AS. Role of Mitochondrial RNA
494 Polymerase in the Toxicity of Nucleotide Inhibitors of Hepatitis C Virus. *Antimicrob Agents*
495 *Chemother* 2016;**60**:806-817.
- 496 13. Lund KC, Wallace KB. Adenosine 3',5'-cyclic monophosphate (cAMP)-dependent
497 phosphoregulation of mitochondrial complex I is inhibited by nucleoside reverse
498 transcriptase inhibitors. *Toxicol Appl Pharmacol* 2008;**226**:94-106.
- 499 14. Gao RY, Mukhopadhyay P, Mohanraj R, Wang H, Horvath B, Yin S, Pacher P. Resveratrol
500 attenuates azidothymidine-induced cardiotoxicity by decreasing mitochondrial reactive
501 oxygen species generation in human cardiomyocytes. *Molecular medicine reports*
502 2011;**4**:151-155.
- 503 15. Bansal M. Cardiovascular disease and COVID-19. *Diabetes Metab Syndr* 2020;**14**:247-250.
- 504 16. Zhou F, Yu T, Du R, Fan G, Liu Y, Liu Z, Xiang J, Wang Y, Song B, Gu X, Guan L, Wei
505 Y, Li H, Wu X, Xu J, Tu S, Zhang Y, Chen H, Cao B. Clinical course and risk factors for
506 mortality of adult inpatients with COVID-19 in Wuhan, China: a retrospective cohort study.
507 *Lancet* 2020;**395**:1054-1062.
- 508 17. Shi S, Qin M, Shen B, Cai Y, Liu T, Yang F, Gong W, Liu X, Liang J, Zhao Q, Huang H,
509 Yang B, Huang C. Association of Cardiac Injury With Mortality in Hospitalized Patients
510 With COVID-19 in Wuhan, China. *JAMA Cardiol* 2020.

- 511 18. Sharma A, Garcia G, Jr., Wang Y, Plummer JT, Morizono K, Arumugaswami V, Svendsen
512 CN. Human iPSC-Derived Cardiomyocytes Are Susceptible to SARS-CoV-2 Infection. *Cell*
513 *Rep Med* 2020;**1**:100052.
- 514 19. Yang L, Han Y, Nilsson-Payant BE, Gupta V, Wang P, Duan X, Tang X, Zhu J, Zhao Z,
515 Jaffre F, Zhang T, Kim TW, Harschnitz O, Redmond D, Houghton S, Liu C, Naji A, Ciceri
516 G, Guttikonda S, Bram Y, Nguyen DT, Cioffi M, Chandar V, Hoagland DA, Huang Y,
517 Xiang J, Wang H, Lyden D, Borczuk A, Chen HJ, Studer L, Pan FC, Ho DD, tenOever BR,
518 Evans T, Schwartz RE, Chen S. A Human Pluripotent Stem Cell-based Platform to Study
519 SARS-CoV-2 Tropism and Model Virus Infection in Human Cells and Organoids. *Cell Stem*
520 *Cell* 2020;**27**:125-136 e127.
- 521 20. Wichmann D, Sperhake JP, Lutgehetmann M, Steurer S, Edler C, Heinemann A, Heinrich F,
522 Mushumba H, Kniep I, Schroder AS, Burdelski C, de Heer G, Nierhaus A, Frings D,
523 Pfefferle S, Becker H, Brederke-Wiedling H, de Weerth A, Paschen HR, Sheikhzadeh-
524 Eggers S, Stang A, Schmiedel S, Bokemeyer C, Addo MM, Aepfelbacher M, Puschel K,
525 Kluge S. Autopsy Findings and Venous Thromboembolism in Patients With COVID-19: A
526 Prospective Cohort Study. *Annals of internal medicine* 2020;**173**:268-277.
- 527 21. Bose RJC, McCarthy JR. Direct SARS-CoV-2 infection of the heart potentiates the
528 cardiovascular sequelae of COVID-19. *Drug Discov Today* 2020.
- 529 22. Bojkova D, Wagner JUG, Shumliakivska M, Aslan GS, Saleem U, Hansen A, Luxan G,
530 Gunther S, Pham MD, Krishnan J, Harter PN, Ermel UH, Frangakis AS, Milting H, Zeiher
531 AM, Klingel K, Cinatl J, Dendorfer A, Eschenhagen T, Tschöpe C, Ciesek S, Dimmeler S.
532 SARS-CoV-2 infects and induces cytotoxic effects in human cardiomyocytes. *Cardiovasc*
533 *Res* 2020.
- 534 23. Gopal R, Marinelli MA, Alcorn JF. Immune Mechanisms in Cardiovascular Diseases
535 Associated With Viral Infection. *Frontiers in immunology* 2020;**11**:570681.

- 536 24. Magadum A, Kishore R. Cardiovascular Manifestations of COVID-19 Infection. *Cells*
537 2020;**9**.
- 538 25. Xie J, Covassin N, Fan Z, Singh P, Gao W, Li G, Kara T, Somers VK. Association Between
539 Hypoxemia and Mortality in Patients With COVID-19. *Mayo Clinic proceedings Mayo*
540 *Clinic* 2020;**95**:1138-1147.
- 541 26. Karbalai Saleh S, Oraii A, Soleimani A, Hadadi A, Shajari Z, Montazeri M, Moradi H,
542 Talebpour M, Sadat Naseri A, Balali P, Akhbari M, Ashraf H. The association between
543 cardiac injury and outcomes in hospitalized patients with COVID-19. *Internal and*
544 *emergency medicine* 2020;**15**:1415-1424.
- 545 27. Musunuru K, Sheikh F, Gupta RM, Houser SR, Maher KO, Milan DJ, Terzic A, Wu JC,
546 American Heart Association Council on Functional G, Translational B, Council on
547 Cardiovascular Disease in the Y, Council on C, Stroke N. Induced Pluripotent Stem Cells
548 for Cardiovascular Disease Modeling and Precision Medicine: A Scientific Statement From
549 the American Heart Association. *Circ Genom Precis Med* 2018;**11**:e000043.
- 550 28. Gintant G, Burr ridge P, Gepstein L, Harding S, Herron T, Hong C, Jalife J, Wu JC. Use of
551 Human Induced Pluripotent Stem Cell-Derived Cardiomyocytes in Preclinical Cancer Drug
552 Cardiotoxicity Testing: A Scientific Statement From the American Heart Association. *Circ*
553 *Res* 2019;**125**:e75-e92.
- 554 29. Magdy T, Schuldt AJT, Wu JC, Bernstein D, Burr ridge PW. Human Induced Pluripotent
555 Stem Cell (hiPSC)-Derived Cells to Assess Drug Cardiotoxicity: Opportunities and
556 Problems. *Annu Rev Pharmacol Toxicol* 2018;**58**:83-103.
- 557 30. Paik DT, Chandy M, Wu JC. Patient and Disease-Specific Induced Pluripotent Stem Cells
558 for Discovery of Personalized Cardiovascular Drugs and Therapeutics. *Pharmacological*
559 *reviews* 2020;**72**:320-342.
- 560 31. Poon EN, Luo XL, Webb SE, Yan B, Zhao R, Wu SCM, Yang Y, Zhang P, Bai H, Shao J,
561 Chan CM, Chan GC, Tsang SY, Gundry RL, Yang HT, Boheler KR. The cell surface

- 562 marker CD36 selectively identifies matured, mitochondria-rich hPSC-cardiomyocytes. *Cell*
563 *Res* 2020;**30**:626-629.
- 564 32. Choi SW, Shin JS, Park SJ, Jung E, Park YG, Lee J, Kim SJ, Park HJ, Lee JH, Park SM,
565 Moon SH, Ban K, Go YY. Antiviral activity and safety of remdesivir against SARS-CoV-2
566 infection in human pluripotent stem cell-derived cardiomyocytes. *Antiviral Res*
567 2020:104955.
- 568 33. Wong CK, Luk HK, Lai WH, Lau YM, Zhang RR, Wong AC, Lo GC, Chan KH, Hung IF,
569 Tse HF, Woo PC, Lau SK, Siu CW. Human-Induced Pluripotent Stem Cell-Derived
570 Cardiomyocytes Platform to Study SARS-CoV-2 Related Myocardial Injury. *Circulation*
571 *journal : official journal of the Japanese Circulation Society* 2020.
- 572 34. Yang X, Rodriguez ML, Leonard A, Sun L, Fischer KA, Wang Y, Ritterhoff J, Zhao L,
573 Kolwicz SC, Jr., Pabon L, Reinecke H, Sniadecki NJ, Tian R, Ruohola-Baker H, Xu H,
574 Murry CE. Fatty Acids Enhance the Maturation of Cardiomyocytes Derived from Human
575 Pluripotent Stem Cells. *Stem cell reports* 2019;**13**:657-668.
- 576 35. Weber N, Schwanke K, Greten S, Wendland M, Iorga B, Fischer M, Geers-Knorr C,
577 Hegermann J, Wrede C, Fiedler J, Kempf H, Franke A, Piep B, Pfanne A, Thum T, Martin
578 U, Brenner B, Zweigerdt R, Kraft T. Stiff matrix induces switch to pure beta-cardiac myosin
579 heavy chain expression in human ESC-derived cardiomyocytes. *Basic Res Cardiol*
580 2016;**111**:68.
- 581 36. Jorgensen SCJ, Kebriaei R, Dresser LD. Remdesivir: Review of Pharmacology, Pre-clinical
582 Data, and Emerging Clinical Experience for COVID-19. *Pharmacotherapy* 2020;**40**:659-
583 671.
- 584 37. Ni HM, Williams JA, Ding WX. Mitochondrial dynamics and mitochondrial quality control.
585 *Redox Biol* 2015;**4**:6-13.
- 586 38. Archer SL. Mitochondrial dynamics--mitochondrial fission and fusion in human diseases. *N*
587 *Engl J Med* 2013;**369**:2236-2251.

- 588 39. Smirnova E, Griparic L, Shurland DL, van der Bliek AM. Dynamin-related protein Drp1 is
589 required for mitochondrial division in mammalian cells. *Mol Biol Cell* 2001;**12**:2245-2256.
- 590 40. Cassidy-Stone A, Chipuk JE, Ingerman E, Song C, Yoo C, Kuwana T, Kurth MJ, Shaw JT,
591 Hinshaw JE, Green DR, Nunnari J. Chemical inhibition of the mitochondrial division
592 dynamin reveals its role in Bax/Bak-dependent mitochondrial outer membrane
593 permeabilization. *Developmental cell* 2008;**14**:193-204.
- 594 41. Wu D, Dasgupta A, Chen KH, Neuber-Hess M, Patel J, Hurst TE, Mewburn JD, Lima PDA,
595 Alizadeh E, Martin A, Wells M, Snieckus V, Archer SL. Identification of novel dynamin-
596 related protein 1 (Drp1) GTPase inhibitors: Therapeutic potential of Drpitor1 and Drpitor1a
597 in cancer and cardiac ischemia-reperfusion injury. *FASEB J* 2020;**34**:1447-1464.
- 598 42. Sheahan TP, Sims AC, Graham RL, Menachery VD, Gralinski LE, Case JB, Leist SR, Pyrc
599 K, Feng JY, Trantcheva I, Bannister R, Park Y, Babusis D, Clarke MO, Mackman RL,
600 Spahn JE, Palmiotti CA, Siegel D, Ray AS, Cihlar T, Jordan R, Denison MR, Baric RS.
601 Broad-spectrum antiviral GS-5734 inhibits both epidemic and zoonotic coronaviruses. *Sci*
602 *Transl Med* 2017;**9**.
- 603 43. Akinci E, Cha M, Lin L, Yeo G, Hamilton MC, Donahue CJ, Bermudez-Cabrera HC,
604 Zanetti LC, Chen M, Barkal SA, Khowpinitchai B, Chu N, Velimirovic M, Jodhani R, Fife
605 JD, Sovrovic M, Cole PA, Davey RA, Cassa CA, Sherwood RI. Elucidation of remdesivir
606 cytotoxicity pathways through genome-wide CRISPR-Cas9 screening and transcriptomics.
607 *bioRxiv* 2020.
- 608 44. Xu Y, Barauskas O, Kim C, Babusis D, Murakami E, Korniyeyev D, Lee G, Stepan G,
609 Perron M, Bannister R, Schultz BE, Sakowicz R, Porter D, Cihlar T, Feng JY. Off-Target In
610 Vitro Profiling Demonstrates that Remdesivir Is a Highly Selective Antiviral Agent.
611 *Antimicrob Agents Chemother* 2021;**65**.
- 612 45. Tchesnokov EP, Feng JY, Porter DP, Gotte M. Mechanism of Inhibition of Ebola Virus
613 RNA-Dependent RNA Polymerase by Remdesivir. *Viruses* 2019;**11**.

- 614 46. Gharanei M, Hussain A, Janneh O, Maddock H. Attenuation of doxorubicin-induced
615 cardiotoxicity by mdivi-1: a mitochondrial division/mitophagy inhibitor. *PLoS One*
616 2013;**8**:e77713.
- 617 47. Ishikita A, Matoba T, Ikeda G, Koga J, Mao Y, Nakano K, Takeuchi O, Sadoshima J,
618 Egashira K. Nanoparticle-Mediated Delivery of Mitochondrial Division Inhibitor 1 to the
619 Myocardium Protects the Heart From Ischemia-Reperfusion Injury Through Inhibition of
620 Mitochondria Outer Membrane Permeabilization: A New Therapeutic Modality for Acute
621 Myocardial Infarction. *Journal of the American Heart Association* 2016;**5**.
- 622 48. Maneechote C, Palee S, Kerdphoo S, Jaiwongkam T, Chattipakorn SC, Chattipakorn N.
623 Differential temporal inhibition of mitochondrial fission by Mdivi-1 exerts effective
624 cardioprotection in cardiac ischemia/reperfusion injury. *Clinical science* 2018;**132**:1669-
625 1683.
- 626 49. Givvimani S, Munjal C, Tyagi N, Sen U, Metreveli N, Tyagi SC. Mitochondrial
627 division/mitophagy inhibitor (Mdivi) ameliorates pressure overload induced heart failure.
628 *PLoS One* 2012;**7**:e32388.
- 629 50. Tobin MJ, Laghi F, Jubran A. Why COVID-19 Silent Hypoxemia Is Baffling to Physicians.
630 *Am J Respir Crit Care Med* 2020;**202**:356-360.
- 631 51. Touafchia A, Bagheri H, Carrie D, Durrieu G, Sommet A, Chouchana L, Montastruc F.
632 Serious bradycardia and remdesivir for coronavirus 2019 (COVID-19): a new safety
633 concerns. *Clinical microbiology and infection : the official publication of the European*
634 *Society of Clinical Microbiology and Infectious Diseases* 2021.
- 635 52. Pallotto C, Suardi LR, Gabbuti A, Esperti S, Mecocci L, Blanc P. Potential remdesivir-
636 related transient bradycardia in patients with coronavirus disease 2019 (COVID-19). *J Med*
637 *Virol* 2021;**93**:2631-2634.
- 638 53. Spinner CD, Gottlieb RL, Criner GJ, Arribas Lopez JR, Cattelan AM, Soriano Viladomiu A,
639 Ogbuagu O, Malhotra P, Mullane KM, Castagna A, Chai LYA, Roestenberg M, Tsang

- 640 OTY, Bernasconi E, Le Turnier P, Chang SC, SenGupta D, Hyland RH, Osinusi AO, Cao
641 H, Blair C, Wang H, Gaggar A, Brainard DM, McPhail MJ, Bhagani S, Ahn MY, Sanyal
642 AJ, Huhn G, Marty FM, Investigators G-U-. Effect of Remdesivir vs Standard Care on
643 Clinical Status at 11 Days in Patients With Moderate COVID-19: A Randomized Clinical
644 Trial. *Jama* 2020;**324**:1048-1057.
- 645 54. Goldman JD, Lye DCB, Hui DS, Marks KM, Bruno R, Montejano R, Spinner CD, Galli M,
646 Ahn MY, Nahass RG, Chen YS, SenGupta D, Hyland RH, Osinusi AO, Cao H, Blair C,
647 Wei X, Gaggar A, Brainard DM, Towner WJ, Munoz J, Mullane KM, Marty FM, Tashima
648 KT, Diaz G, Subramanian A, Investigators G-U-. Remdesivir for 5 or 10 Days in Patients
649 with Severe Covid-19. *N Engl J Med* 2020.
- 650 55. Poon E, Keung W, Liang Y, Ramalingam R, Yan B, Zhang S, Chopra A, Moore J, Herren
651 A, Lieu DK, Wong HS, Weng Z, Wong OT, Lam YW, Tomaselli GF, Chen C, Boheler KR,
652 Li RA. Proteomic Analysis of Human Pluripotent Stem Cell-Derived, Fetal, and Adult
653 Ventricular Cardiomyocytes Reveals Pathways Crucial for Cardiac Metabolism and
654 Maturation. *Circ Cardiovasc Genet* 2015;**8**:427-436.
- 655 56. Poon E, Yan B, Zhang S, Rushing S, Keung W, Ren L, Lieu DK, Geng L, Kong CW, Wang
656 J, Wong HS, Boheler KR, Li RA. Transcriptome-guided functional analyses reveal novel
657 biological properties and regulatory hierarchy of human embryonic stem cell-derived
658 ventricular cardiomyocytes crucial for maturation. *PLoS One* 2013;**8**:e77784.
- 659 57. Poon EN, Hao B, Guan D, Jun Li M, Lu J, Yang Y, Wu B, Wu SC, Webb SE, Liang Y,
660 Miller AL, Yao X, Wang J, Yan B, Boheler KR. Integrated transcriptomic and regulatory
661 network analyses identify microRNA-200c as a novel repressor of human pluripotent stem
662 cell-derived cardiomyocyte differentiation and maturation. *Cardiovasc Res* 2018;**114**:894-
663 906.
- 664 58. Boheler KR, Poon EN. Cell surface markers for immunophenotyping human pluripotent
665 stem cell-derived cardiomyocytes. *Pflugers Arch* 2021.

- 666 59. Puntmann VO, Carerj ML, Wieters I, Fahim M, Arendt C, Hoffmann J, Shchendrygina A,
667 Escher F, Vasa-Nicotera M, Zeiher AM, Vehreschild M, Nagel E. Outcomes of
668 Cardiovascular Magnetic Resonance Imaging in Patients Recently Recovered From
669 Coronavirus Disease 2019 (COVID-19). *JAMA Cardiol* 2020;**5**:1265-1273.
- 670 60. Sahakijpijarn S, Moon C, Koleng JJ, Christensen DJ, Williams Iii RO. Development of
671 Remdesivir as a Dry Powder for Inhalation by Thin Film Freezing. *Pharmaceutics* 2020;**12**.
- 672
- 673

674 **Figure Legends**

675

676 **Figure 1. Remdesivir induced mitochondrial dysfunction in hiPSC-CMs.**

677 Human iPSC-CMs were treated with indicated doses of remdesivir under normoxic or hypoxic
678 conditions for 3 days. (A) Mitochondrial redox activity was measured using the PrestoBlue assay,
679 n=11. (B) Seahorse metabolic flux analysis revealed altered metabolic profiles upon remdesivir
680 treatment. Oxygen consumption rate=OCR, OGN=oligomycin, FCCP=Carbonyl cyanide p-trifluoro-
681 methoxyphenyl hydrazone, Rot/AA=Rotenone+actimycin. Key parameters are summarised and
682 graphed: Normoxia: n=5, Hypoxia: n=6. (C) Confocal fluorescence images of mitotracker dye
683 staining (red) revealed disturbed mitochondrial organisation in hiPSC-CMs treated with remdesivir.
684 Hoescht nuclear staining is in blue. The proportion of cells with elongated (asterick), punctate
685 (arrowhead) and perinuclear (arrow) mitochondria were quantified, n=7. Statistical significance was
686 calculated relative to control cells using the one-way ANOVA with Dunnett's multiple comparisons
687 test for (A, B), and two-way ANOVA with Sidak's multiple comparisons test for (C), *p<0.05,
688 **p<0.01, ***p<0.001, ****p<0.0001. Scale bar = 10µm.

689

690 **Figure 2. Remdesivir perturbed the expression of genes important for mitochondrial function.**

691 Human iPSC-CMs were treated with indicated doses of remdesivir under normoxic or hypoxic
692 conditions for 3 days. The expression of selected genes were measured by qRT-PCR, normalised to
693 B2M, n=5. Statistical significance was calculated using the one-way ANOVA with Dunnett's multiple
694 comparisons relative to control cells *p<0.05, **p<0.01, ***p<0.001.

695

696 **Figure 3. Remdesivir induced sarcomeric disarray in hiPSC-CMs.**

697 (A) Confocal images of hiPSC-CMs showing MLC2V-eGFP signal in green, Hoescht nuclear
698 staining in blue. Representative images of 6 independent batches of cells are shown. Control hiPSC-
699 CMs have densely-packed, striated MLC2V-eGFP signal, reflecting its localization to the thick

700 filaments of sarcomeres, and was absent from the Z-disk and I-band. Sparse and truncated sarcomeres
701 (arrowheads), patchy MLC2V-eGFP signal with no or poorly discernible organisation (arrows) could
702 be detected in cells treated with high doses of remdesivir. (B) The proportion of cells with condensed
703 nuclei was assessed among control cells and cells treated with the indicated doses of remdesivir.
704 Statistical significance was examined using the one-way ANOVA test and no statistically significant
705 difference was detected among the samples, n=8.

706

707 **Figure 4. Remdesivir altered the electrophysiological properties of hiPSC-CMs.**

708 Human iPSC-CMs were treated with/without 2.5 μ M of remdesivir under normoxic conditions for 3
709 days. The electrophysiological properties were measured using patch-clamp analysis. (A)
710 Representative tracings and (B) action potential parameters of control and remdesivir-treated cells
711 are shown. Statistical significance was calculated relative to control cells using the student's T-test,
712 n=14 *p<0.05, **p<0.01.

713

714 **Figure 5. Remdesivir induced persistent mitochondrial and structural abnormalities in hiPSC-**
715 **CMs.**

716 (A) Human iPSC-CMs were treated with indicated doses of remdesivir under normoxic (blue) or
717 hypoxic (yellow) conditions for 3 days, and allowed to recover in the absence of remdesivir for 3
718 more days under normoxic conditions. (B) Mitochondrial redox activity was measured using the
719 PrestoBlue assay, n=8. (C) Confocal fluorescence images of mitotracker dye staining (red) revealed
720 elongated mitochondria (asterick) in most control cells, while the majority of remdesivir treated cells
721 had punctate mitochondria (arrowhead). Perinuclear mitochondria (arrow) were enriched in cells
722 treated with 12.5 μ M of remdesivir, n=5. Hoescht nuclear staining is in blue. (D) Confocal images of
723 hiPSC-CMs showing MLC2V-eGFP signal in green, Hoescht nuclear staining in blue. Sparse and
724 truncated sarcomeres (arrowheads), patchy MLC2V-eGFP signal with no or poorly discernible
725 organisation (arrows) could be detected in cells treated with remdesivir. Dotted arrow indicates a cell

726 with brightly stained, condensed nuclei. (E) Quantification of cells with condensed nuclei, n=6.
727 Statistical significance was calculated relative to control cells using the one-way ANOVA with
728 Dunnett's multiple comparisons test for (B) and (E), and two-way ANOVA with Sidak's multiple
729 comparisons test for (C), *p<0.05, **p<0.01, ***p<0.001, ****p<0.0001. Scale bar = 10µm.

730

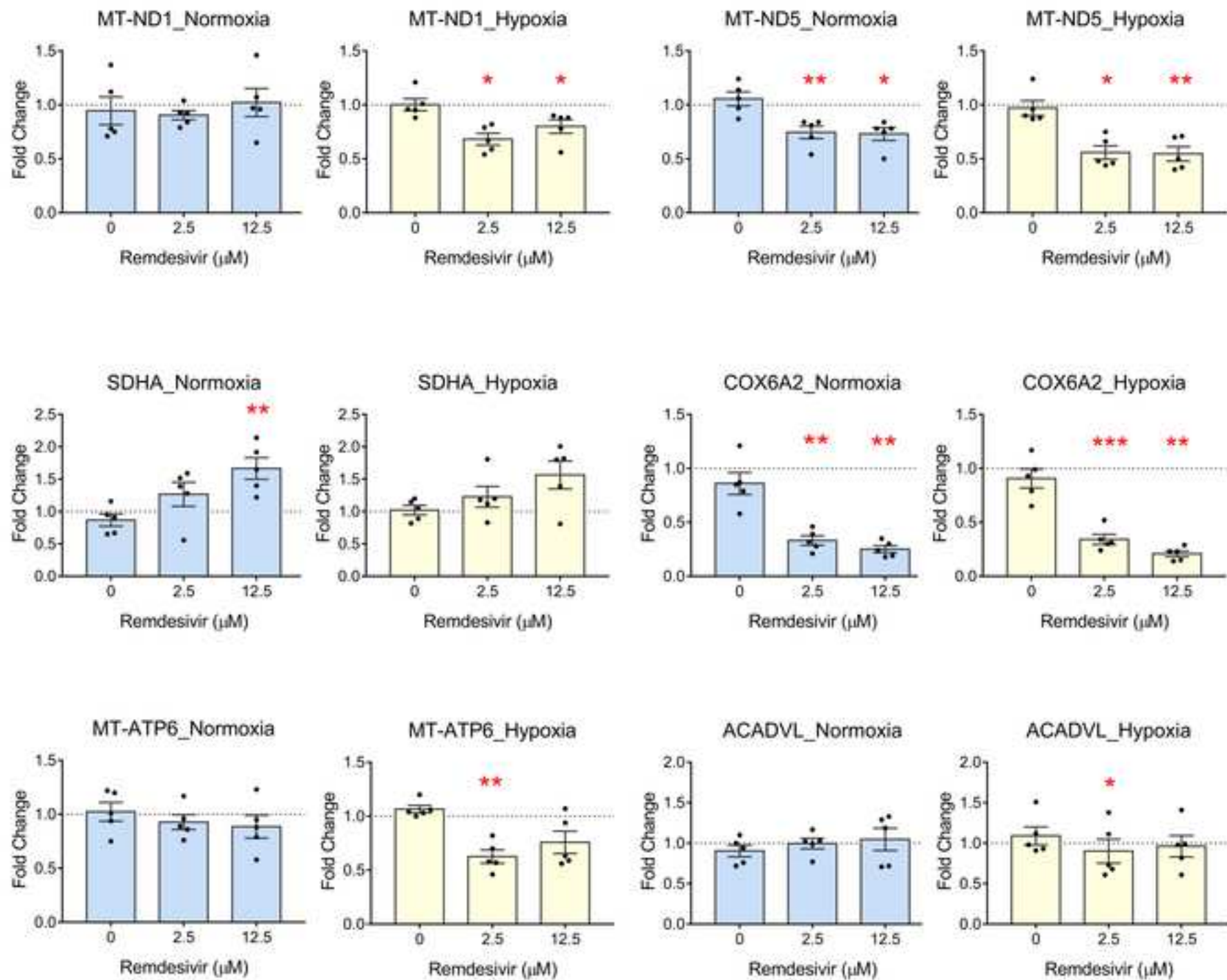
731 **Figure 6. An inhibitor of mitochondrial fission protected against remdesivir induced**
732 **cardiotoxicity.**

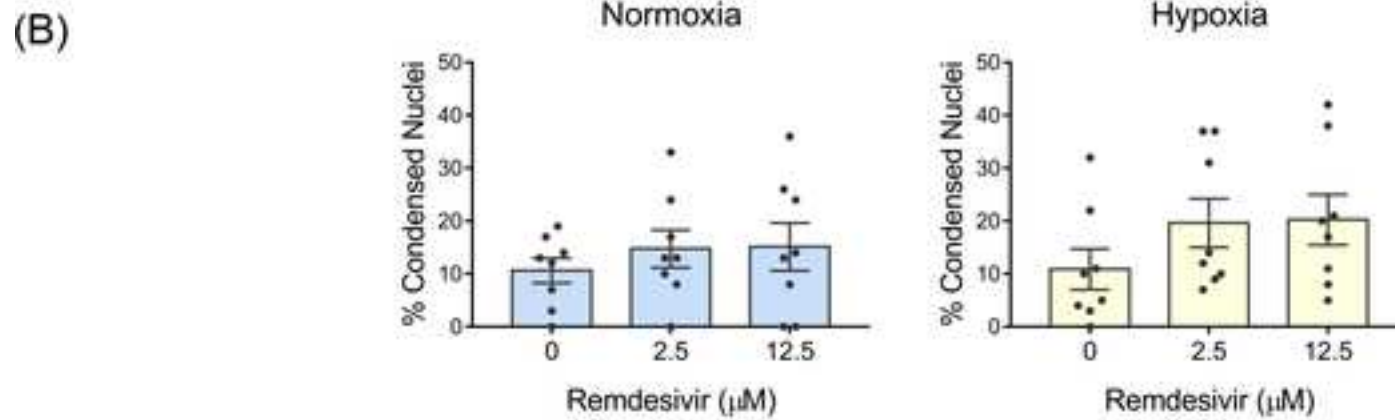
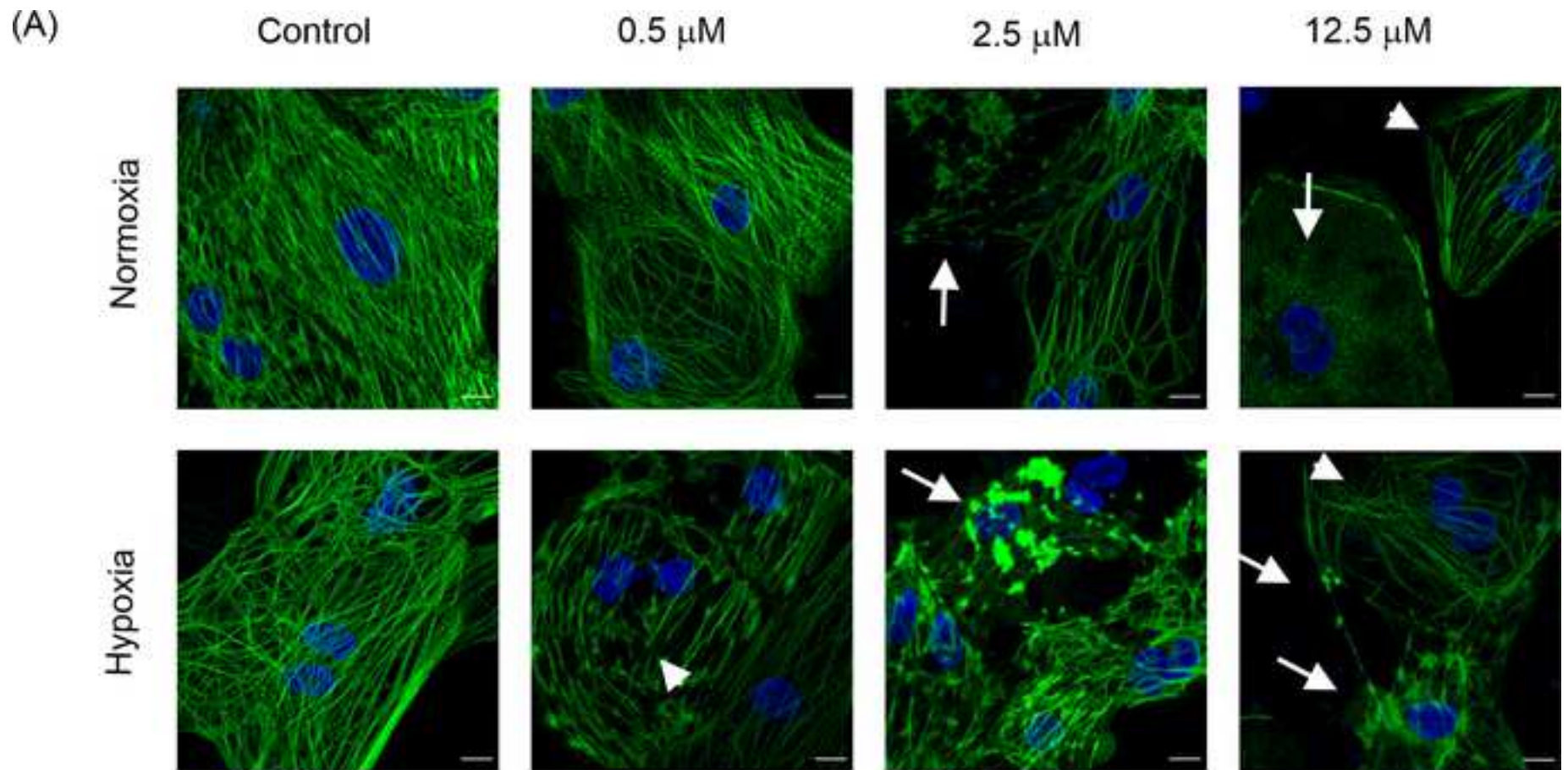
733 Human iPSC-CMs were treated with indicated doses of remdesivir under normoxic or hypoxic
734 conditions, in the presence/absence of mdivi-1 (MD, 15 µM). (A) Mitochondrial redox activity was
735 measured using the PrestoBlue assay, n=7. (B) Mitochondrial morphology was assessed using
736 mitotracker staining in red, Hoescht nuclear staining in blue, n=6 for normoxia and n=5 for hypoxia.
737 MD co-treatment with 2.5 µM remdesivir increased the proportion of cells with elongated
738 mitochondria (asterisk), while cells treated with remdesivir alone displayed mostly punctate
739 (arrowhead) and perinuclear (arrow) mitochondria. (C) Confocal images of hiPSC-CMs showing
740 MLC2V-eGFP signal in green. Sparse and truncated sarcomeres (arrowheads), patchy MLC2V-eGFP
741 signal with no or poorly discernible organisation (arrows) were enriched in cells with remdesivir
742 alone, while MD co-treatment resulted in more striated sarcomeres. Statistical significance was
743 calculated using the (A) one-way ANOVA with Sidak's multiple comparisons test against cells treated
744 with remdesivir alone without MD, and two-way ANOVA with Sidak's multiple comparisons test
745 against cells treated with remdesivir alone without MD for (B). *p<0.05, **p<0.01. Scale bar = 10µm.

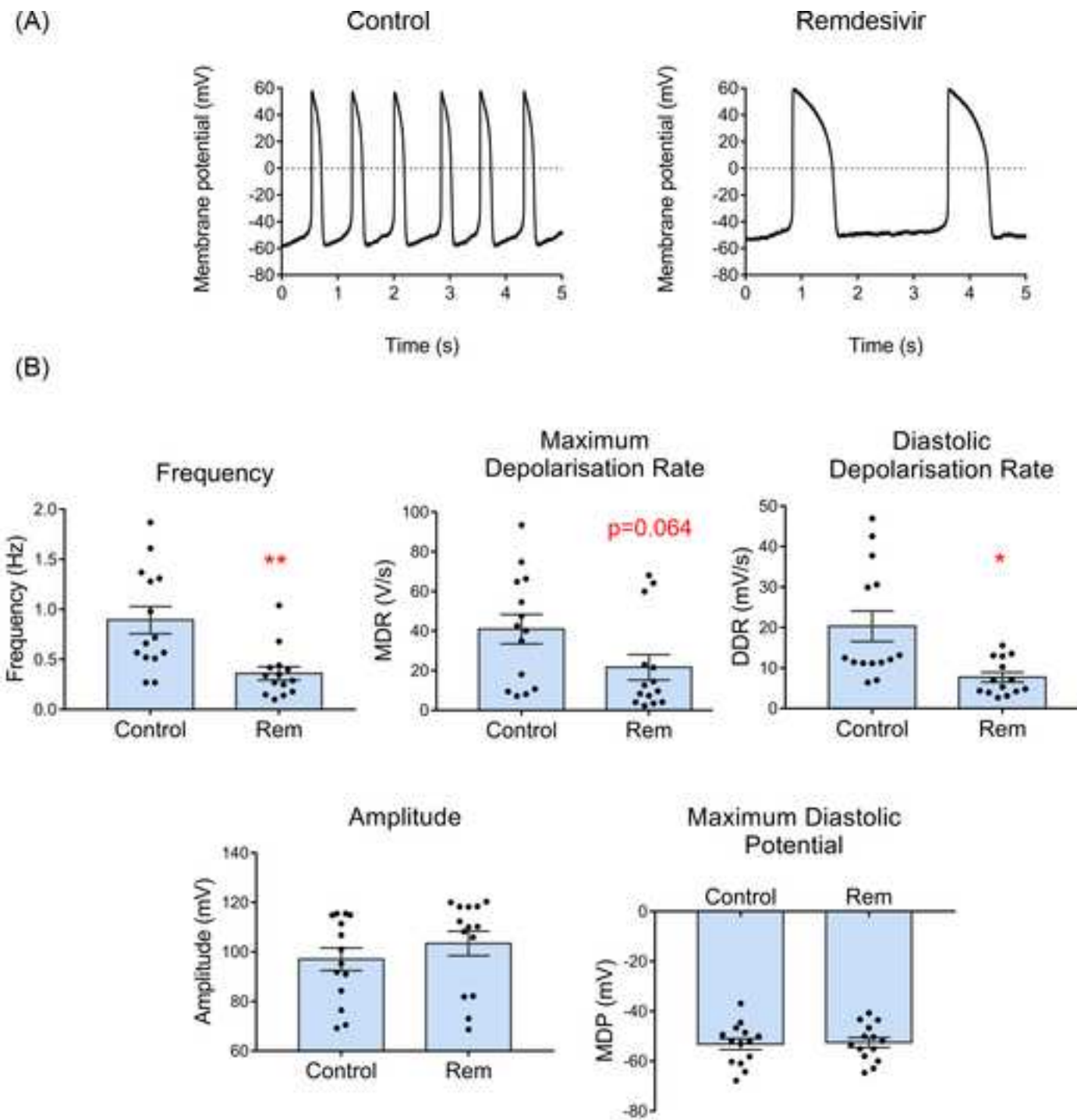
746

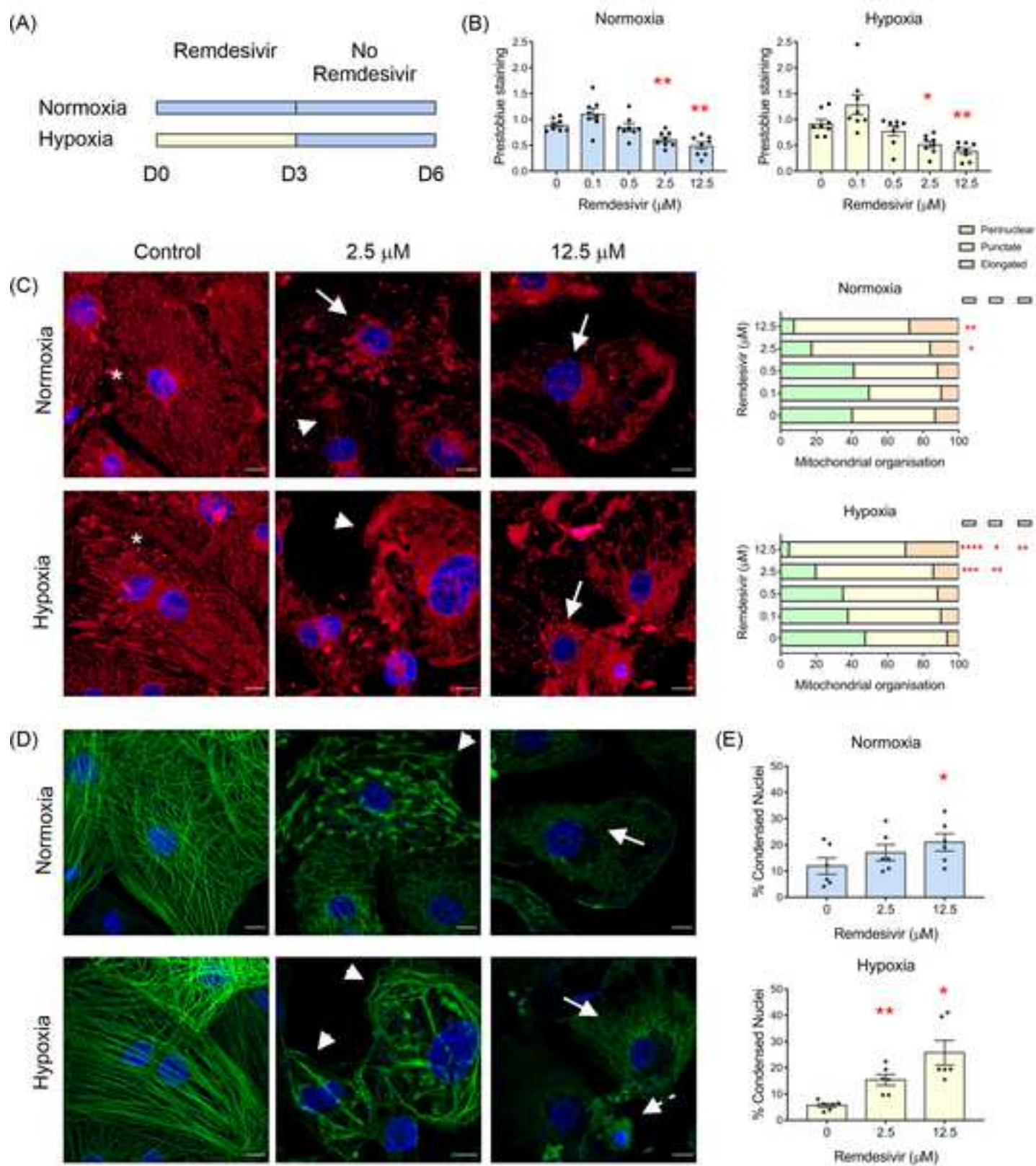
747

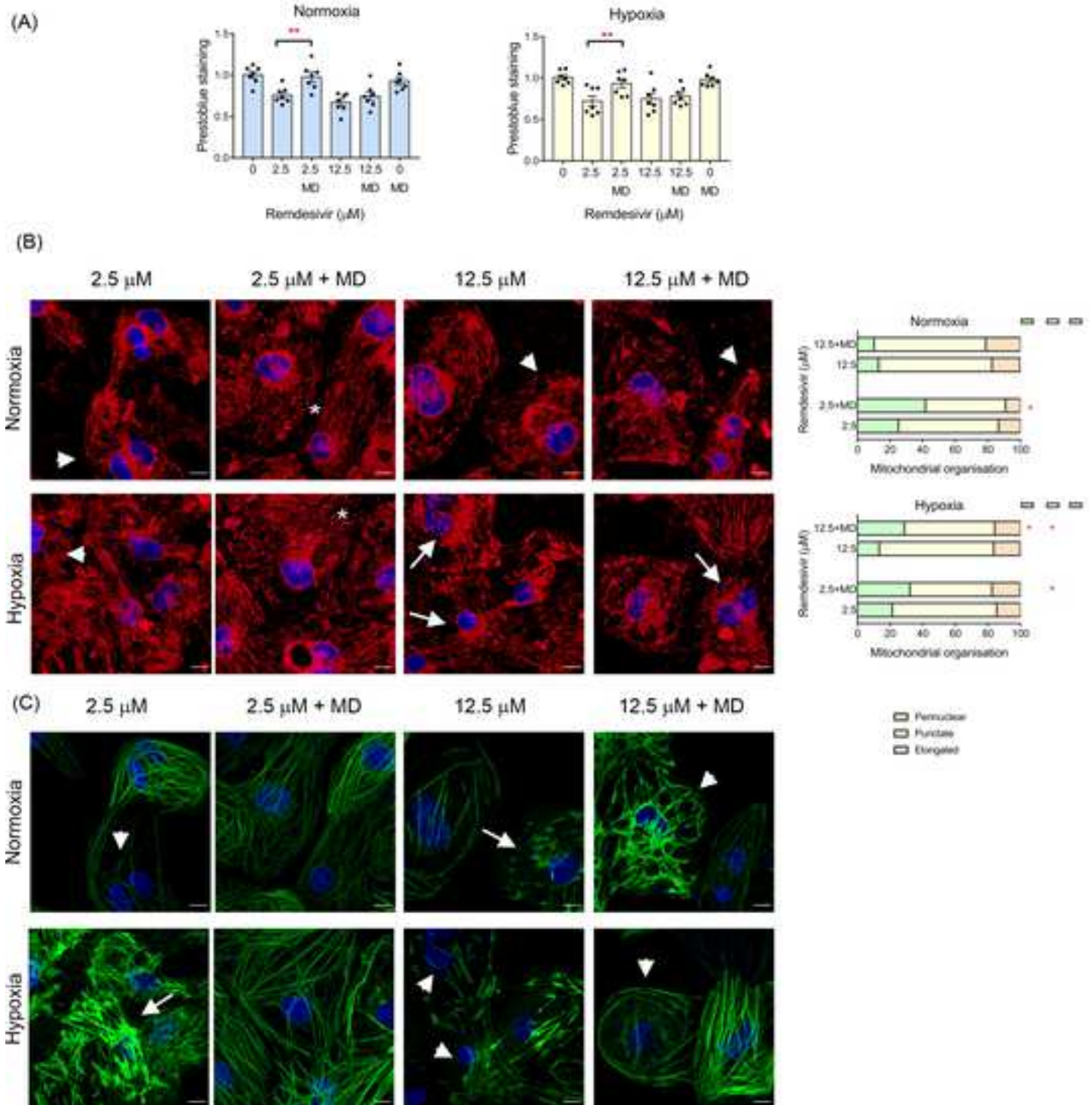
748











Remdesivir

